A Space–Time Correlation Model for Multielement Antenna Systems in Mobile Fading Channels

Ali Abdi, *Member, IEEE* and Mostafa Kaveh, *Fellow, IEEE*

***Abstract*—Analysis and design of multielement antenna systems in mobile fading channels require a model for the space–time cross correlation among the links of the underlying multiple-input multiple-output (MIMO) channel. In this paper, we propose a general space–time cross-correlation function for mobile frequency nonselective Rice fading MIMO channels, in which various parameters of interest such as the angle spreads at the base station and the user, the distance between the base station and the user, mean directions of the signal arrivals, array configurations, and Doppler spread are all taken into account. The new space–time cross-correlation function includes all the relevant parameters of the MIMO fading channel in a clean compact form, suitable for both mathematical analysis and numerical calculations/simulations. It also covers many known correlation models as special cases. We demonstrate the utility of the new space–time correlation model by clarifying the limitations of a widely accepted correlation model for MIMO fading channels. As another application, we quantify the impact of nonisotropic scattering around the user, on the capacity of a MIMO fading channel.**

***Index Terms*—Fading channels, MIMO systems, multielement antenna systems, multipath channels, nonisotropic scattering, Rice fading, Shannon capacity, space–time correlation.**

I. Introduction

In RECENT years the application of antenna arrays for wireless cellular systems has received much attention, as they improve the coverage and quality of such systems by combating interference and fading. It has also been shown that by exploiting antenna arrays at both the transmitters and receivers, the capacity of wireless channels can be increased significantly [1], [2]. An antenna array can be defined as a spatio-temporal filter, which takes advantage of both time-domain and space-domain signal characteristics. The need for efficient joint use of time-domain and space–domain data using multielement antenna systems has generated new paradigms such as space–time coding [3] and space–time signal processing techniques. Needless to say, new space–time channel models have to be developed as well. Since the second-order statistics of the channel characterize the basic structure of stochastic wireless fading channels, we need a spatio-temporal cross-correlation function, that enables us to study the basic impact of the random multipath fading channel on the performance of space–time solutions, implemented by multielement antenna systems.

According to the wireless connection scheme between a base station (BS) and a user in macrocells, depicted in Fig. 1, the BS, which is not surrounded by many local scatterers, receives the signal primarily from a particular direction through a narrow beamwidth. On the other hand, the local scatterers around the user may give rise to different modes of signal propagation toward the user. In the general scenario of nonisotropic scattering, which corresponds to directional signal reception, the user receives the signal only from particular directions (see Fig. 2). The special case of isotropic scattering is shown in Fig. 3, where the user receives signals from all directions with equal probabilities. The isotropic scattering model, also known as the Clarke's model, corresponds to the uniform distribution for the angle of arrival (AOA). However, empirical measurements [4], [5] have shown that the AOA distribution of waves impinging the user is more likely to be nonuniform. The nonuniform distribution of the AOA can significantly affect the performance of array based techniques, as the AOA statistics determine the cross correlation among the array elements. Examples regarding the noticeable impact of the AOA characteristics on the asymptotic efficiency of decision-directed and decorrelating multiuser-multichannel array detectors with imperfect channel estimates, and the bit error rate of a maximal ratio array combiner are discussed in [6].

The application of von Mises angular distribution for the nonuniform AOA was first proposed in [8], where the temporal correlation function for a single antenna receiver was derived and successfully fitted to measured data, as an extension of the Clarke's classic model. The temporal correlation model of [8] has been generalized to a spatio-temporal model [6], [7] suitable for a multielement antenna receiver. The specific mathematical form of the von Mises distribution has resulted in an easy-to-use and closed-form expression for the space–time correlation function in [6] and [7], which has also shown good fit to the published correlation data in the literature [6].

In what follows, we derive a closed-form, easy-to-use, and mathematically tractable expression for the space–time cross correlation between the links of a frequency nonselective multiple-input multiple-output (MIMO) Rice wireless fading channel with multielement transmit and receive antennas, where nonisotropic scattering around the user is modeled by the von Mises distribution. The effect of the mobility of the user (the Doppler spread) is also considered, which is particularly useful as the next generation of cellular system are expected to work for very high speed users at high data rates. As we will

Manuscript received February 1, 2001; revised September 29, 2001. This work was supported in part by the National Science Foundation under the Wireless Initiative Program, Grant 9979443. This paper was presented at IEEE International Conference Acoustics, Speech, and Signal Processing, Salt Lake City, Utah, 2001.

A. Abdi is with the Department of Electrical and Computer Engineering, New Jersey Institute of Technology, Newark, NJ 07102 USA (e-mail: ali.abdi@njit.edu).

M. Kaveh is with the Department of Electrical and Computer Engineering, University of Minnesota, Minneapolis, MN 55455 USA (e-mail: kaveh@ece.umn.edu).

Publisher Item Identifier S 0733-8716(02)03296-1.

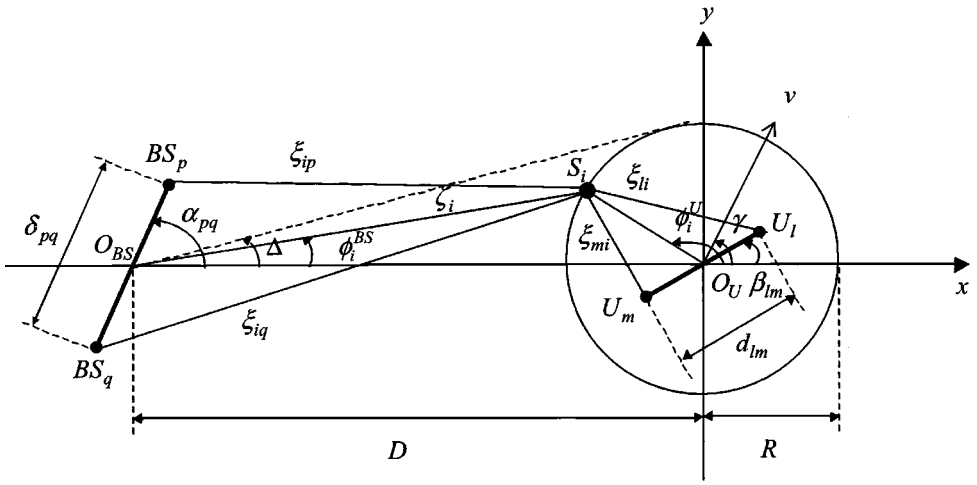

Fig. 1. Geometrical configuration of a 2×2 channel with local scatterers around the mobile user (two-element arrays at the BS and the user).

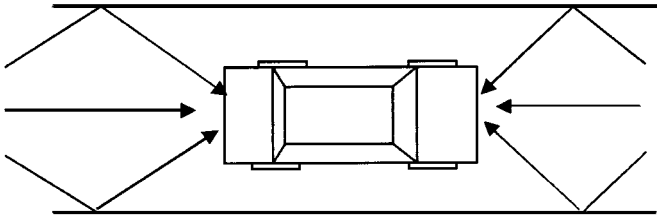

Fig. 2. Non-isotropic scattering in a narrow street.

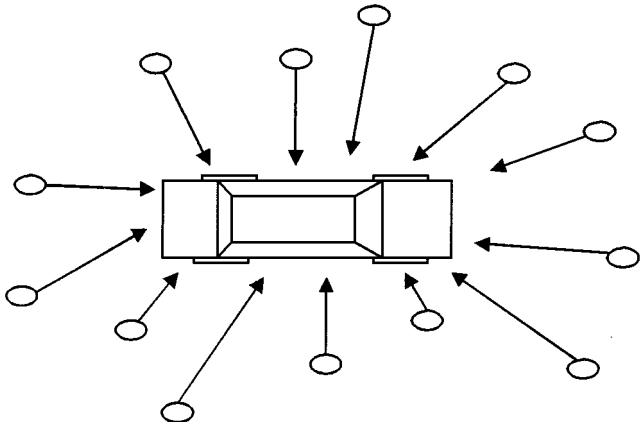

Fig. 3. Isotropic scattering in an open area (circles are scatterers).

see later, the proposed model includes many known correlation functions as special cases.

There are numerous applications of the proposed correlation model in multielement antenna systems with space–time modems, such as the joint selection of antenna spacing and interleaving depth [9], channel interpolation using the Wiener filter [10], calculation of capacity [11]–[19], optimum combining to suppress the interferers, and combat the fading of the desired user [20], and so forth. In this paper, we use the new correlation model to study the capacity of the MIMO frequency nonselective Rice channel, where the fixed user experiences nonisotropic scattering. Our numerical results shed more light on the maximum achievable data rates in multielement antenna systems, where the user receives signal from particular directions. This capacity case study also demonstrates the key role of the proposed correlation model in quantifying the effect of propagation channel characteristics on the ultimate limits of communications using array-based systems.

II. The MIMO Frequency Nonselective Rice Channel

Consider the multielement antenna system configuration shown in Fig. 1, first proposed in [11], where the BS and the user have n_{BS} and n_U omnidirectional antenna elements, respectively. Obviously, in Fig. 1, we have uniform linear arrays with $n_{\mathrm{BS}} = n_U = 2$ (a 2×2 MIMO channel), which constitutes the basic structure of multielement antenna systems with arbitrary array configurations. Our convention for numbering the antenna elements is such that $1 \leq l \leq m \leq n_U$ and $1 \leq p \leq q \leq n_{\mathrm{BS}}$. The BS receives the signal through the narrow beamwidth Δ, while the user receives the signal from a large number of surrounding local scatterers, impinging the user from different directions. We assume that the waves are planar and only single scattering occurs. The ith scatterer is represented by S_i, D is the distance between the BS and the user, and R is the radius of the ring of scatterers. Clearly, Δ, R, and D are related through $\tan(\Delta) = R/D$. We also assume that a line-of-sight (LOS), which is not considered in [11], may exist between any pair of BS-user antenna elements, as shown in Fig. 4. The LOS paths are not shown on Fig. 1, to keep the figure easier to read. Notice that for a particular pair of the BS-user antenna elements, a strong specular component may appear in place of the LOS component. However, since the geometrical representation of a specular component is not as straightforward as a LOS component, which is easily depicted in Fig. 4 by a straight line between any pair of BS-user antenna elements, we have excluded specular components from our model.

Let us consider the downlink with no transmit beamforming. Let $s_p(t)$ represent the complex envelope of the signal transmitted from the pth BS array element and $r_l(t)$ the complex envelope of the signal received by the lth user's array element. For the frequency nonselective communication link between the element BS_p and the element U_l, the complex lowpass equivalent channel response $h_{lp}(t)$ appears as a multiplicative factor. Note that such a *link* comprises of many *paths* that can be drawn

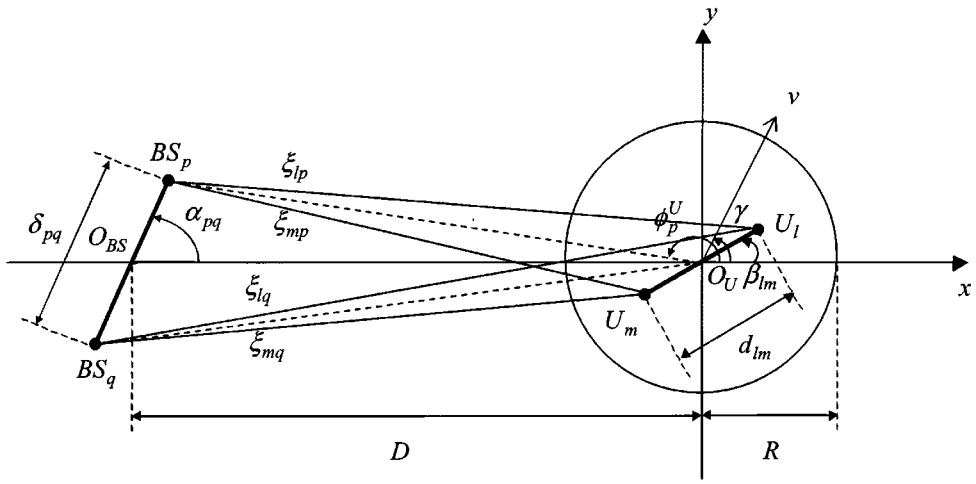

Fig. 4. The LOS paths in the 2×2 channel of Fig. 1.

from BS_p to U_l through the ring of local scatterers enclosing the user, as well as the LOS path. Based on the vector notations $\boldsymbol{s}(t) = [s_1(t) \dots s_{n_{\mathrm{BS}}}(t)]'$ and $\boldsymbol{r}(t) = [r_1(t) \dots r_{n_U}(t)]'$, with $\cdot'$ as the transpose operator, the input–output equation for the frequency nonselective MIMO fading channel can be written as

$$\boldsymbol{r}(t) = \boldsymbol{H}(t)\boldsymbol{s}(t) + \boldsymbol{n}(t) \tag{1}$$

where $\boldsymbol{H}(t)$ is the $n_U \times n_{\mathrm{BS}}$ channel matrix complex envelope such that $[\boldsymbol{H}(t)]_{lp} = h_{lp}(t)$, and $\boldsymbol{n}(t)$ stands for the complex envelope of the additive white Gaussian noise (AWGN) with zero mean vector and the diagonal covariance matrix, i.e., $E[\boldsymbol{n}(t)\boldsymbol{n}^{\#}(t)] = P_{\mathrm{noise}}\boldsymbol{I}_{n_U}$, where P_{noise} is the noise power at each receiver, $\boldsymbol{I}_{n_U}$ is the $n_U \times n_U$ real identity matrix, and $^{\#}$ denotes the transpose conjugate operator. The dependence of $\boldsymbol{H}(t)$ on time is a result of user mobility (Doppler effect). This implies that we have taken into account the effect of channel time selectivity. Needless to say, the space selectivity of the channel is also considered through the realistic assumption of nonisotropic scattering and nonuniform distribution of AOA [21].

In the channel model depicted in Figs. 1 and 4, the ring of scatterers is assumed to be fixed (independent of time), and the motion of the user is characterized by its speed v and the direction of the motion γ. These assumptions are necessary for obtaining a stationary space–time correlation function. The same assumptions can be found, for example, in [22] and [23, Section 2.1] for the temporal correlation model, and in [9] and [24] for the spatio-temporal correlation model. Clearly, depending on the user's speed, the spatio-temporal correlation function derived in the sequel will be accurate only over a time duration that is much smaller than R/ν. Moving scatterers further complicate the modeling problem. The reader is referred to [25] and [26], where some theoretical and simulation results are presented regarding the impact of a rotating ring of scatterers, surrounding a single-antenna user, on the BS array correlation.

For a unit transmit power, suppose the power transferred through the BS_p–U_t link is Ω_{lp}, i.e., $\Omega_{lp} = E\left[|h_{lp}(t)|^2\right] \leq 1$. Based on Figs. 1 and 4, the channel gain $h_{lp}(t)$ can be represented by $h_{lp}(t) = h_{lp}^{\mathrm{DIF}}(t) + h_{lp}^{\mathrm{LOS}}(t)$. The plane waves emitted from the array element BS_p travel over paths with different lengths and after being scattered by the local scatterers around the mobile user, impinge the array element U_l from different directions. Mathematical representation of this propagation mechanism results in the following expressions for the diffuse and the LOS components, identified by the superscripts DIF and LOS, respectively

$$\begin{aligned} h_{lp}^{\mathrm{DIF}}(t) = & \sqrt{\frac{\Omega_{lp}}{K_{lp}+1}} \lim_{N\to\infty} \frac{1}{\sqrt{N}} \sum_{i=1}^{N} g_i \\ & \times \exp\left\{ j\psi_i - \frac{j2\pi}{\lambda}\left[\xi_{ip}\left(\phi_i^U\right) + \xi_{li}\left(\phi_i^U\right)\right] \right. \\ & \left. + j2\pi f_D\left[\cos\left(\phi_i^U - \gamma\right)\right] t \right\} \end{aligned} \tag{2}$$

$$\begin{aligned} h_{lp}^{\mathrm{LOS}}(t) = & \sqrt{\frac{\Omega_{lp}K_{lp}}{K_{lp}+1}} \\ & \times \exp\left\{ -\frac{j2\pi}{\lambda}\xi_{lp} + j2\pi f_D\left[\cos\left(\phi_p^U - \gamma\right)\right] t \right\}. \end{aligned} \tag{3}$$

As becomes clear soon, $h_{lp}^{\mathrm{DIF}}(t)$ is random process, while $h_{lp}^{\mathrm{LOS}}(t)$ is deterministic. In the above formulas, K_{lp} is the Rice factor of the BS_p–U_l link, defined as the ratio of the LOS component power to the diffuse component power, i.e., $K_{lp} = \left|h_{lp}^{\mathrm{LOS}}(t)\right|^2 / E\left[\left|h_{lp}^{\mathrm{DIF}}(t)\right|^2\right]$. Moreover, N is the number of independent scatterers S_i around the user, g_i represents the amplitude of the wave scattered by the ith scatterer toward the user such that $N^{-1}\sum_{i=1}^{N} E\left[g_i^2\right] = 1$ as $N \to \infty$. ψ_i denotes the phase shift introduced by the ith scatterer, ξ_{ip} and ξ_{li} are the distances shown in Fig. 1, which are functions of ϕ_i^U, the AOA of the wave traveling from the ith scatterer toward the user, λ is the wavelength, $j^2 = -1$, $f_D = \nu/\lambda$ is the maximum Doppler shift, and finally, ξ_{lp} and ϕ_p^U denote the length and the direction of the LOS path between BS_p and U_l in Fig. 4, respectively. The set $\{g_i\}_{i=1}^{\infty}$ consists of independent positive random variables with finite variances, independent of $\{\psi_i\}_{i=1}^{\infty}$. It is reasonable to assume that $\{\psi_i\}_{i=1}^{\infty}$ are independent and identically distributed (iid) random variables with uniform distributions over $[0, 2\pi)$. The

particular representation of $h_{lp}^{\rm DIF}(t)$ and $h_{lp}^{\rm LOS}(t)$ in terms of K_{lp}, together with the assumption of $N^{-1}\sum_{i=1}^{N} E\left[g_i^2\right] \to 1$ as $N \to \infty$, guarantees that $E\left[|h_{lp}(t)|^2\right] = \Omega_{lp}$.

According to the statistical properties of the channel described above, central limit theorem implies that $h_{lp}(t)$ is a lowpass nonzero-mean complex Gaussian process. Hence, the envelope $|h_{lp}(t)|$ is a Rice process. In other words, our model represents a MIMO frequency nonselective Rice fading channel. For $K_{lp} = 0$, i.e., no LOS, the model reduces to a MIMO frequency nonselective Rayleigh fading channel. Obviously, $h_{lp}^{\rm DIF}(t)$ is a lowpass zero-mean complex Gaussian process, while $h_{lp}^{\rm LOS}(t)$ is a deterministic process.

III. The New Space–Time Cross-Correlation Function

Let us define the space–time cross correlation between the gains of the two arbitrary communication links $h_{lp}(t)$ and $h_{mq}(t)$ as $\rho_{lp,mq}(\tau,t) = E\left[h_{lp}(t)h_{mq}^*(t+\tau)\right]/\sqrt{\Omega_{lp}\Omega_{mq}}$, where * is the complex conjugate. If we further define $\rho_{lp,mq}^{\rm DIF}(\tau,t) = E\left[h_{lp}^{\rm DIF}(t)h_{mq}^{\rm DIF*}(t+\tau)\right]/\sqrt{\Omega_{lp}\Omega_{mq}}$ and $\rho_{lp,mq}^{\rm LOS}(\tau,t) = h_{lp}^{\rm LOS}(t)h_{mq}^{\rm LOS*}(t+\tau)/\sqrt{\Omega_{lp}\Omega_{mq}}$, then it is easy to verify that $\rho_{lp,mq}(\tau,t) = \rho_{lp,mq}^{\rm DIF}(\tau,t) + \rho_{lp,mq}^{\rm LOS}(\tau,t)$, as $h_{lp}^{\rm DIF}(t)$ and $h_{mq}^{\rm DIF}(t)$ are zero-mean processes. In Sections III-A and B, we derive exact and appropriate approximate expressions for the diffuse and the LOS parts of $\rho_{lp,mq}(\tau,t)$. The approximations generally hold when $D \gg R \gg \max(\delta_{pq}, d_{lm})$, which corresponds to the small values of Δ. According to the experiments conducted at different locations and frequencies [22, p. 65], [24], [27]–[31], the angle spread Δ at the BS is generally small for macrocells in urban, suburban, and rural areas, most often less than 15°, and in some cases very small, less than 5°. These empirical observations justify the simple but useful approximate results for $\rho_{lp,mq}^{\rm DIF}(\tau,t)$ and $\rho_{lp,mq}^{\rm LOS}(\tau,t)$, derived in the sequel. However, for those cases where Δ is not small, more complex but exact results are given as well.

A. Cross-Correlation Function of the Diffuse Component

Based on the statistical properties of $\{g_i\}_{i=1}^{\infty}$ and $\{\psi_i\}_{i=1}^{\infty}$, discussed in Section II, the space–time cross correlation between $h_{lp}^{\rm DIF}(t)$ and $h_{mq}^{\rm DIF}(t)$, according to (2), can be written as

$$\begin{aligned}\rho_{lp,mq}^{\rm DIF}(\tau,t) =& \rho_{lp,mq}^{\rm DIF}(\tau)\\ =& \frac{1}{\sqrt{(K_{lp}+1)(K_{mq}+1)}} \lim_{N\to\infty} \frac{1}{N}\sum_{i=1}^{N} E[g_i^2]\\ &\times \exp\left\{-\frac{j2\pi}{\lambda}\left(\xi_{ip} - \xi_{iq} + \xi_{li} - \xi_{mi}\right)\right.\\ &\left.-j2\pi f_D\left[\cos(\phi_i^U - \gamma)\right]\tau\right\}. \end{aligned} \tag{4}$$

According to (4), the total diffuse power of the link ${\rm BS}_p - U_l$, scattered by all the scatterers toward the user's lth element is given by

$$E\left[\left|h_{lp}^{\rm DIF}(t)\right|^2\right] = \Omega_{lp}/(K_{lp}+1)$$

also obvious from (2). For large N, the small contribution of the ith scatterer, out of the total $\Omega_{lp}/(K_{lp}+1)$, is proportional to $E\left[g_i^2\right]/N$. This is equal to the infinitesimal power coming from the differential angle $d\phi^U$ with probability $f\left(\phi_i^U\right)$, i.e., $E\left[g_i^2\right]/N = f\left(\phi_i^U\right)d\phi^U$ (see [22, p. 23]), where $f(\phi^U)$ is the pdf of the AOA seen by the user. Therefore, (4) can be written in the following integral form

$$\begin{aligned}\rho_{lp,mq}^{\rm DIF}(\tau) =& \frac{1}{\sqrt{(K_{lp}+1)(K_{mq}+1)}}\\ &\times \int_{-\pi}^{\pi} \exp\left\{-\frac{j2\pi}{\lambda}\right.\\ &\qquad\times\left(\xi_{\phi^U p} - \xi_{\phi^U q} + \xi_{l\phi^U} - \xi_{m\phi^U}\right)\\ &\qquad\left.-j2\pi f_D\left[\cos(\phi^U - \gamma)\right]\tau\right\}\\ &\times f(\phi^U)d\phi^U \end{aligned} \tag{5}$$

where $\xi_{\phi^U p}$ is the length of the path between the antenna element ${\rm BS}_p$ and the point on the ring of scatterers, determined by ϕ^U, and so on. For the special case of $K_{lp} = K_{mq} = 0$, $f(\phi^U) = 1/(2\pi)$, and $f_D = 0$, (5) simplifies to (5) in [11].

For a given $f(\phi^U)$, (5) needs to be calculated numerically, according to the following relations derived based on the application of the law of cosines in appropriate triangles

$$\begin{aligned}\xi_{\phi^U p}^2 =& \frac{\delta_{pq}^2}{4} + \zeta_{\phi^U}^2 - \delta_{pq}\zeta_{\phi^U}\cos\left(\alpha_{pq} - \phi_{\phi^U}^{\rm BS}\right)\\ \xi_{\phi^U q}^2 =& \frac{\delta_{pq}^2}{4} + \zeta_{\phi^U}^2 + \delta_{pq}\zeta_{\phi^U}\cos\left(\alpha_{pq} - \phi_{\phi^U}^{\rm BS}\right)\\ \xi_{l\phi^U}^2 =& \frac{d_{lm}^2}{4} + R^2 - d_{lm}R\cos\left(\phi^U - \beta_{lm}\right)\\ \xi_{m\phi^U}^2 =& \frac{d_{lm}^2}{4} + R^2 + d_{lm}R\cos\left(\phi^U - \beta_{lm}\right)\end{aligned} \tag{6}$$

where the interpretations of ζ_{ϕ^U} and $\phi_{\phi^U}^{\rm BS}$ are clear from their counterparts ζ_i and $\phi_i^{\rm BS}$ in Fig. 1, respectively. For a given ϕ^U, $\phi_{\phi^U}^{\rm BS}$ and ζ_{ϕ^U} can be determined according the following equations, derived through the application of the law of sines in the triangle $O_{\rm BS}S_iO_U$

$$\frac{D}{\sin\left(\phi^U - \phi_{\phi^U}^{\rm BS}\right)} = \frac{R}{\sin\left(\phi_{\phi^U}^{\rm BS}\right)} = \frac{\zeta_{\phi^U}}{\sin(\phi^U)}. \tag{7}$$

However, the appropriate assumption of $D \gg R \gg \max(\delta_{pq}, d_{lm})$ for many practical cases of interest, which also implies that Δ is small, simplifies the equations drastically. We use the approximate relations $\sqrt{1+\chi} \approx 1 + \chi/2$, $\sin\chi \approx \chi$, and $\cos\chi \approx 1$, when χ is small. To begin with, the first equation in (7) yields $\phi_{\phi^U}^{\rm BS} \approx \Delta\sin(\phi^U)$, as $\phi_{\phi^U}^{\rm BS}$ and $\Delta \approx R/D$ are small. Consequently, the equations in (6) can be written as

$$\begin{aligned}\xi_{\phi^U p} \approx& \zeta_{\phi^U} - \frac{\delta_{pq}}{2}\left[\cos(\alpha_{pq}) + \Delta\sin(\alpha_{pq})\sin(\phi^U)\right]\\ \xi_{\phi^U q} \approx& \zeta_{\phi^U} + \frac{\delta_{pq}}{2}\left[\cos(\alpha_{pq}) + \Delta\sin(\alpha_{pq})\sin(\phi^U)\right]\\ \xi_{l\phi^U} \approx& R - \frac{d_{lm}}{2}\cos(\phi^U - \beta_{lm})\\ \xi_{m\phi^U} \approx& R + \frac{d_{lm}}{2}\cos(\phi^U - \beta_{lm}).\end{aligned} \tag{8}$$

Substitution of (8) into (5) yields

$$\rho_{lp,mq}^{\mathrm{DIF}}(\tau) \approx \frac{1}{\sqrt{(K_{lp}+1)(K_{mq}+1)}} \exp\left\{\frac{j2\pi\delta_{pq}\cos(\alpha_{pq})}{\lambda}\right\} \times \int_{-\pi}^{\pi} \exp\left\{\frac{j2\pi}{\lambda}\left[\delta_{pq}\Delta\sin(\alpha_{pq})\sin(\phi^U) + d_{lm}\cos(\phi^U-\beta_{lm})\right] - j2\pi f_D\left[\cos\left(\phi^U-\gamma\right)\right]\tau\right\} \times f(\phi^U)d\phi^U. \quad (9)$$

The approximate cross-correlation expression given in (9) holds for any angular PDF $f(\phi^U)$. Here we employ the von Mises PDF [8]

$$f(\phi^U) = \frac{\exp[\kappa\cos(\phi^U-\mu)]}{2\pi I_0(\kappa)}, \quad \phi^U \in [-\pi,\pi) \quad (10)$$

where $I_0(.)$ is the zeroth-order modified Bessel function, $\mu \in [-\pi,\pi)$ accounts for the mean direction of AOA seen by the user, and $\kappa \geq 0$ controls the width of AOA [8]. For $\kappa = 0$ (isotropic scattering) we have $f(\phi^U) = 1/(2\pi)$, while for $\kappa = \infty$ (extremely nonisotropic scattering) the von Mises PDF becomes a Dirac delta function, concentrated at $\phi^U = \mu$. For the empirical justifications of the von Mises PDF for the AOA around a single antenna receiver in urban and suburban areas, the reader may refer to [8]. Several applications are also discussed in [32] and [33], that show how the von Mises PDF results in simple mathematically tractable formulas for the AOA-related channel parameters, which significantly facilitate system analysis and design.

To simplify the notation, we define $a = 2\pi f_D\tau$, $b_{lm} = 2\pi d_{lm}/\lambda$, and $c_{pq} = 2\pi\delta_{pq}/\lambda$. By inserting (10) into (9), and calculating the integral, exactly, according to [34, eq. 3.338-4, p. 357]

$$\int_{-\pi}^{\pi} \exp(x\sin z + y\cos z)dz = 2\pi I_0\left(\sqrt{x^2+y^2}\right) \quad (11)$$

we obtain the following key result after some algebraic manipulations

$$\rho_{lp,mq}^{\mathrm{DIF}}(\tau) \approx \frac{1}{\sqrt{(K_{lp}+1)(K_{mq}+1)}} \frac{\exp[jc_{pq}\cos(\alpha_{pq})]}{I_0(\kappa)} \times I_0\Big(\{\kappa^2 - a^2 - b_{lm}^2 - c_{pq}^2\Delta^2\sin^2(\alpha_{pq}) + 2ab_{lm}\cos(\beta_{lm}-\gamma) + 2c_{pq}\Delta\sin(\alpha_{pq}) \times [a\sin(\gamma) - b_{lm}\sin(\beta_{lm})] - j2\kappa[a\cos(\mu-\gamma) - b_{lm}\cos(\mu-\beta_{lm}) - c_{pq}\Delta\sin(\alpha_{pq})\sin(\mu)]\}^{1/2}\Big). \quad (12)$$

The proposed space–time cross-correlation function for the diffuse component, valid for small Δ, includes all the relevant parameters of the MIMO frequency nonselective fading channel with multielement antennas in a compact form, suitable for both mathematical analysis and numerical calculations/simulations. The compact form of (12) provides computational advantages over the simulation-based correlation models such as the one in [35], as they may require a large number of simulation runs to realize the statistical characteristics of the channel. In what follows and for $K_{lp} = K_{mq} = 0$, we show how most of the existing correlation models can be identified as special cases of our generic MIMO model in (12).

The simplest special case of (12) is Clarke's temporal correlation model $J_0(2\pi f_D\tau)$ [22], obtained for $d_{11} = \delta_{11} = 0$ (single transmit–receive antennas) and $\kappa = 0$ (isotropic scattering around the user), where $J_0(.)$ is the zeroth-order Bessel function. For the case of nonisotropic scattering around the user, $\kappa \neq 0$, with $\gamma = 180°$, (12) reduces to the temporal correlation model in (2) of [8], $I_0\left(\sqrt{\kappa^2 - 4\pi^2 f_D^2\tau^2 + j4\pi\kappa\cos(\mu)f_D\tau}\right)/I_0(\kappa)$. Remarkably, this correlation model has shown very good fit to the measured data [8].

When the BS has a single antenna, while the user is equipped with a uniform linear array, two models can be identified in the literature. The simpler model is the Lee's spatio-temporal model [36], where the user experiences isotropic scattering. Lee's result can be obtained by substituting $\delta_{11} = 0$, $\kappa = 0$, and $\beta_{lm} = 180°$ into (12), which yields $J_0\left(\sqrt{a^2 + b_{lm}^2 + 2ab_{lm}\cos\gamma}\right)$ (see [36, eqs. (42)–(43)], with f_D changed to $-f_D$). The second spatio-temporal model is the extension of Lee's result, when we have nonisotropic scattering around the user, i.e., $\kappa \neq 0$. In this case, (12) simplifies to the equation at the bottom of the page, originally given in [6, eq. (3)], with f_D replaced by $-f_D$.

On the other hand, when the BS has a uniform linear array and the user has a single antenna, the simplest case could be the spatial model in (7) of [37], $\exp[jc_{pq}\cos(\alpha_{pq})]J_0(c_{pq}\Delta\sin\alpha_{pq})$, obtained by substituting $d_{11} = 0$, $\kappa = 0$, and $f_D = 0$ into (12). Notice that in this model, the stationary user experiences isotropic scattering. By allowing $f_D \neq 0$, this model can be extended to the spatio-temporal model of [9], which can be written as $\exp[jc_{pq}\cos(\alpha_{pq})]$ $J_0\left(\sqrt{a^2 + c_{pq}^2\Delta^2\sin^2(\alpha_{pq}) - 2ac_{pq}\Delta\sin(\alpha_{pq})\sin(\gamma)}\right)$. This equation can be derived from (3) of [9], when Δ is small.

In addition to macrocells, the assumption $D \gg R \gg \max(\delta_{pq}, d_{lm})$ in Fig. 1 holds for some microcells, with the same small range of values for the angle spread seen by the BS [29], [38]. Hence, (12) can be used for such microcells as well. For those microcells where the local scattering around the BS is not negligible [39], Fig. 1 and, consequently, (12) should be modified.

$$\frac{I_0\left(\sqrt{\kappa^2 - a^2 - b_{lm}^2 - 2ab_{lm}\cos(\gamma) - j2\kappa\left[a\cos(\mu-\gamma) + b_{lm}\cos(\mu)\right]}\right)}{I_0(\kappa)}$$

The reader might have noted that as a result of the particular setting in Fig. 1, the AOA at the BS is a function of the AOA seen by the user, given in the first equation of (7). Hence, the distribution of ϕ^U determines the distribution of $\phi^{\rm BS}$. However, in order to study the spatial correlation among the elements of a BS antenna array, irrespective of the effect of local scattering around the user, several distributions have been proposed for the distribution of AOA at the BS: power of cosine [24], Gaussian [31], truncated uniform [20], and von Mises distributions [6], [7]. For a comparison between these four distributions, we refer the readers to [6] and [39]. Geometrically based models for the distribution of AOA are discussed in [40].

B. Cross-Correlation Function of the LOS Component

The space–time cross correlation between $h_{lp}^{\rm LOS}(t)$ and $h_{mq}^{\rm LOS}(t)$, according to (3), can be written as

$$\begin{aligned}\rho_{lp,mq}^{\rm LOS}(\tau,t) =&\sqrt{\frac{K_{lp}K_{mq}}{(K_{lp}+1)(K_{mq}+1)}}\\ &\times\exp\left\{-\frac{j2\pi}{\lambda}\left[\xi_{lp}-\xi_{mq}\right]-j2\pi f_D\right.\\ &\times\left[\cos\left(\phi_q^U-\gamma\right)\right]\tau+j2\pi f_D\\ &\left.\times\left[\cos\left(\phi_p^U-\gamma\right)-\cos\left(\phi_q^U-\gamma\right)\right]t\right\}.\end{aligned}\tag{13}$$

Based on the reasonable assumption of $D\gg\delta_{pq}$ in Fig. 4, we obtain $\phi_p^U\approx\phi_q^U\approx 180^\circ$ which in turn simplifies (13) to

$$\begin{aligned}\rho_{lp,mq}^{\rm LOS}(\tau,t)\approx&\rho_{lp,mq}^{\rm LOS}(\tau)\\ =&\sqrt{\frac{K_{lp}K_{mq}}{(K_{lp}+1)(K_{mq}+1)}}\\ &\times\exp\left\{-\frac{j2\pi}{\lambda}\left[\xi_{lp}-\xi_{mq}\right]+j2\pi f_D\cos(\gamma)\tau\right\}.\end{aligned}\tag{14}$$

Application of the law of cosines in the triangles $\mathrm{BS}_pU_lO_U$ and $\mathrm{BS}_qU_mO_U$ yields

$$\begin{aligned}\xi_{lp}^2=&\frac{d_{lm}^2}{4}+\overline{\mathrm{BS}_pO_U}^2-d_{lm}\overline{\mathrm{BS}_pO_U}\cos\left(\phi_p^U-\beta_{lm}\right)\\ \xi_{mq}^2=&\frac{d_{lm}^2}{4}+\overline{\mathrm{BS}_qO_U}^2+d_{lm}\overline{\mathrm{BS}_qO_U}\cos\left(\phi_q^U-\beta_{lm}\right)\end{aligned}\tag{15}$$

where

$$\begin{aligned}\overline{\mathrm{BS}_pO_U}^2=&\frac{\delta_{pq}^2}{4}+D^2-\delta_{pq}D\cos(\alpha_{pq})\\ \overline{\mathrm{BS}_qO_U}^2=&\frac{\delta_{pq}^2}{4}+D^2+\delta_{pq}D\cos(\alpha_{pq}).\end{aligned}\tag{16}$$

Since $\min\left(\overline{\mathrm{BS}_pO_U},\overline{\mathrm{BS}_qO_U}\right)\gg d_{lm}$ and $D\gg\delta_{pq}$, we simplify (15) using the approximate relation $\sqrt{1+\chi}\approx 1+\chi/2$

$$\begin{aligned}\xi_{lp}\approx&D-\frac{\delta_{pq}}{2}\cos(\alpha_{pq})+\frac{d_{lm}}{2}\cos(\beta_{lm})\\ \xi_{mq}\approx&D+\frac{\delta_{pq}}{2}\cos(\alpha_{pq})-\frac{d_{lm}}{2}\cos(\beta_{lm})\end{aligned}\tag{17}$$

in which we have also used the fact that $\phi_p^U\approx\phi_q^U\approx 180^\circ$. Substitution of (17) into (14) results in

$$\begin{aligned}\rho_{lp,mq}^{\rm LOS}(\tau)=&\sqrt{\frac{K_{lp}K_{mq}}{(K_{lp}+1)(K_{mq}+1)}}\\ &\times\exp\left[ja\cos(\gamma)-jb_{lm}\cos(\beta_{lm})\right.\\ &\left.+jc_{pq}\cos(\alpha_{pq})\right].\end{aligned}\tag{18}$$

IV. Separate Versus Joint Correlation Modeling

Based on the two key results derived in the Section III, (12) and (18), the space–time cross-correlation function of the frequency nonselective Rice MIMO channel is given by the summation of these two equations. This cross-correlation function includes all the parameters of the BS and the user's arrays, as well as the distance between the BS and the user and the radius of the ring of scatterers around the user, in a joint fashion. However, either for mathematical convenience [11]–[14], [16], [19], or to have a simple simulation model with parameters taken from measurements [17], [41], it is common to model the cross correlation among the elements of the BS and the user's arrays, separately. The cross correlation among the MIMO channel links is then defined to be [19]

$$\rho_{lp,mq}(\tau)\triangleq\rho_{rp,rq}(\tau)\rho_{ls,ms}(\tau)\tag{19}$$

where $r\in\{1,2,\ldots,n_U\}$ and $s\in\{1,2,\ldots,n_{\rm BS}\}$ are arbitrary antenna indices of the user's and the BS arrays, respectively. Note that (19) does not depend on the indices r and s, i.e., $\rho_{rp,rq}(\tau)$ is the cross correlation between the pth and the qth elements of the BS array, independent of the user's element index r. Likewise, $\rho_{ls,ms}(\tau)$ is the cross correlation between the lth and the mth elements of the user's array, independent of the BS element index s. In other words, the contributions of all the BS antennas to the correlation between the user's antennas are the same, and vice versa (this presumption also holds for our model in (12) and (18)). In the sequel, we show that the commonly-used product model in (19) can be highly inaccurate in comparison with our model and for many cases of practical interest.

To better understand the motivation behind the definition in (19), let us define the correlation matrices of the BS and the user's arrays $\Re_{\rm BS}(\tau)$ and $\Re_U(\tau)$, where $[\Re_{\rm BS}(\tau)]_{pq}=\rho_{rp,rq}(\tau)$, $[\Re_U(\tau)]_{lm}=\rho_{ls,ms}(\tau)$, and r and s are two arbitrary integers defined above. We also define $\mathrm{vec}\{\boldsymbol{H}(t)\}$ as an $n_Un_{\rm BS}\times 1$ vector, constructed by stacking the columns of $\boldsymbol{H}(t)$, the $n_U\times n_{\rm BS}$ channel matrix. If $\boldsymbol{H}(t)=[\boldsymbol{h}_1(t)\boldsymbol{h}_2(t)\ldots\boldsymbol{h}_{n_{\rm BS}}(t)]$, where $\boldsymbol{h}_s(t)$ is an $n_U\times 1$ vector, corresponding to the sth BS antenna element, with the common correlation matrix $\Re_U(\tau)$. Then $\mathrm{vec}\{\boldsymbol{H}(t)\}=\left[\boldsymbol{h'}_1(t)\boldsymbol{h'}_2(t)\ldots\boldsymbol{h'}_{n_{\rm BS}}(t)\right]'$. Based on these definitions, (19) implies that the correlation matrix of $\mathrm{vec}\{\boldsymbol{H}(t)\}$ can be written as [11]

$$E[\mathrm{vec}\{\boldsymbol{H}(t)\}\mathrm{vec}^{\#}\{\boldsymbol{H}(t+\tau)\}]\triangleq\Re_{\rm BS}(\tau)\otimes\Re_U(\tau)\tag{20}$$

where $\otimes$ is the Kronecker product. For two arbitrary matrices $\boldsymbol{A}$ and $\boldsymbol{B}$, this product is defined as [42]

$$\boldsymbol{A}\otimes\boldsymbol{B}\triangleq\begin{bmatrix}[\boldsymbol{A}]_{11}\boldsymbol{B} & [\boldsymbol{A}]_{12}\boldsymbol{B} & \cdots\\ [\boldsymbol{A}]_{21}\boldsymbol{B} & [\boldsymbol{A}]_{22}\boldsymbol{B} & \cdots\\ \vdots & \vdots & \ddots\end{bmatrix}. \tag{21}$$

Equation (20) shows one way of representing the correlation matrix of a matrix variate elliptically contoured distribution, in terms of the correlation matrices of the rows and the columns (see [42, Th. 2.4.1, p. 33 and Corollary 2.4.1.1, p. 34]). For the matrix variate Gaussian distribution as a special case, see p. 34 of [43].

The particular definition of the correlation matrix of $\boldsymbol{H}(t)$ in (20), adopted in [11]–[14], [16], [17], [19], [41], and also in the statistics literature on matrix variate distributions [42], [43], provides us with mathematical convenience and compact notation. However, care should be taken in using (20), as it imposes the particular product form of (19) on the correlation between any two links which originate from different BS antennas and terminate at different user's antennas. The validity of (19) for such links has been studied in [19] using the wire,ess system engineering (WiSE) ray-tracing software simulator. Specifically, for a 2×2 channel with $\tau=0$, they have observed agreement between $\rho_{11,22}(0)$ and $\rho_{11,21}(0)\rho_{11,12}(0)$, over the range of antenna spacings that they considered.

Now we use the new cross-correlation model in (12) and (18), to study the assumption made in (19). For $n_{\rm BS}=n_U=2$, $l=p=1$, and $m=q=2$, let $\tau=0$, $K_{11}=K_{12}=K_{21}=K_{22}=K$, $\alpha_{12}=\beta_{12}=90^\circ$ (parallel arrays), and $\mu=180^\circ$. Then, based on (12) and (18), we obtain

$$\rho_{11,22}(0)=\frac{1}{K+1}\frac{I_0\left(\sqrt{\kappa^2-(b_{12}+c_{12}\Delta)^2}\right)}{I_0(\kappa)}+\frac{K}{K+1} \tag{22}$$

$$\rho_{11,21}(0)=\frac{1}{K+1}\frac{I_0\left(\sqrt{\kappa^2-b_{12}^2}\right)}{I_0(\kappa)}+\frac{K}{K+1} \tag{23}$$

$$\rho_{11,12}(0)=\frac{1}{K+1}\frac{I_0\left(\sqrt{\kappa^2-c_{12}^2\Delta^2}\right)}{I_0(\kappa)}+\frac{K}{K+1}. \tag{24}$$

As expected, $\rho_{11,22}(0)\neq\rho_{11,21}(0)\rho_{11,12}(0)$. Assuming $\Delta=2^\circ$ and $K=2.55\equiv 4$ dB, $\rho_{11,22}(0)$ and the relative difference between $\rho_{11,22}(0)$ and $\rho_{11,21}(0)\rho_{11,12}(0)$, i.e., $\varepsilon\%=100\times[1-\rho_{11,21}(0)\rho_{11,12}(0)/\rho_{11,22}(0)]$, are plotted in Figs. 5 and 6, versus d_{12}/λ and δ_{12}/λ, for $\kappa=3$ and $\kappa=0$, respectively. Note that the angle spread for the user in Fig. 5 is $2/\sqrt{\kappa}\approx 66^\circ$ [8], around the mean AOA of 180°, while the user in Fig. 6 receives signals from all directions uniformly.

As both Figs. 5 and 6 show, the relative difference $\varepsilon\%$ between $\rho_{11,22}(0)$ and $\rho_{11,21}(0)\rho_{11,12}(0)$ is significant over a wide range of antenna spacings. For the nonisotropic scattering scenario of Fig. 5 and at $d_{12}/\lambda=0.7$ and $\delta_{12}/\lambda=20$, we have $\rho_{11,22}(0)\approx 0.7$ and $\varepsilon\%\approx+32$. The case for isotropic scattering scenario in Fig. 6 is even worse. At $d_{12}/\lambda=0.6$ and $\delta_{12}/\lambda=17$, we have $\rho_{11,22}(0)\approx 0.8$ with the relative difference as high as $\varepsilon\%\approx+54$! It has been demonstrated in [44] that fading correlation less than 0.5 results in minor reduction in capacity over the uncorrelated case. Therefore, system modeling based on the product model in (19) and (20) may result in a too optimistic characterization of a more realistic description that can be obtained for a practical multiantenna system.

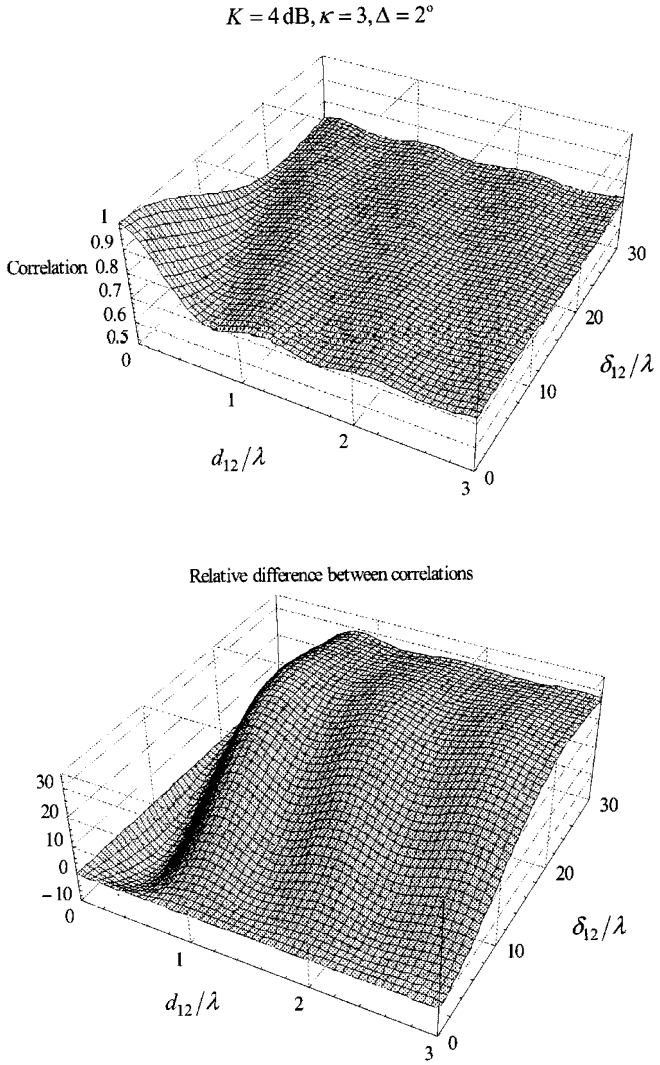

Fig. 5. The correlation $\rho_{11,22}(0)$ (upper) and the relative difference between correlations $100\times[1-\rho_{11,21}(0)\rho_{11,12}(0)/\rho_{11,22}(0)]$ (lower), versus antenna spacings for a 2×2 channel, with nonisotropic scattering around the user ($\kappa=3$), having $2/\sqrt{\kappa}\approx 66^\circ$ and $\Delta=2^\circ$ as the angle spread around the user and the BS, respecitively, with the Rice factor $K=2.55\equiv 4$ dB.

V. Capacity and Nonisotropic Scattering Around the User

To demonstrate the utility of the proposed MIMO correlation model, in this section we study the effect of fading correlation on the capacity of MIMO fading channels. Suppose the underlying frequency nonselective fading channel is such that

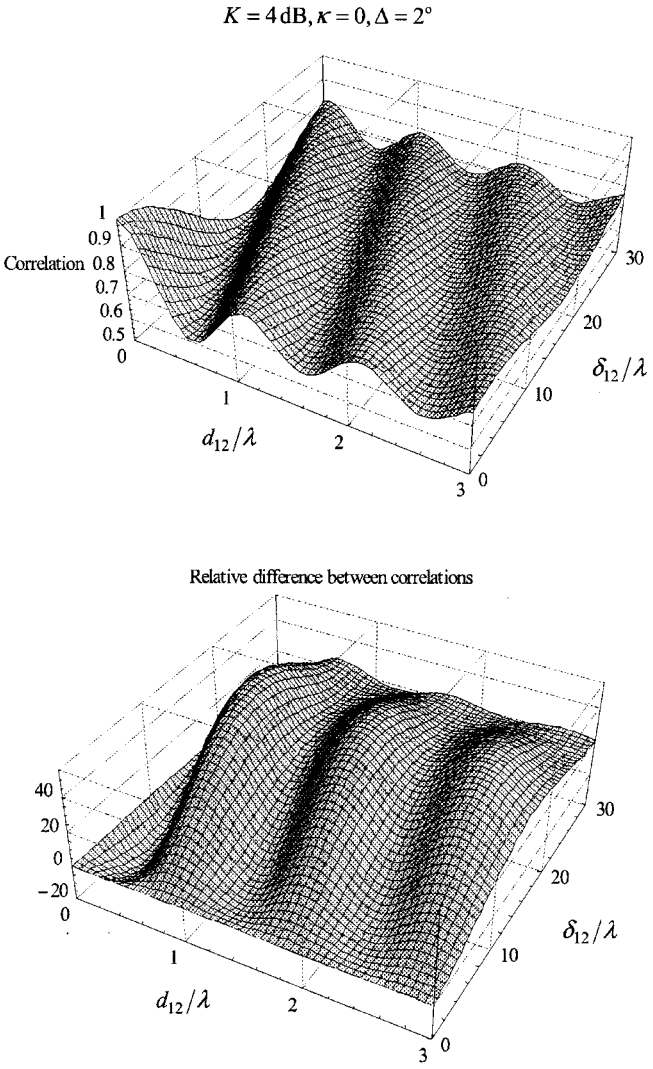

Fig. 6. The correlation $\rho_{11,22}(0)$ (upper) and the relative difference between correlations $100 \times [1 - \rho_{11,21}(0)\rho_{11,12}(0)/\rho_{11,22}(0)]$ (lower), versus antenna spacings for a 2×2 channel, with isotropic scattering around the user ($\kappa = 0$) having $\Delta = 2°$ as the angle spread around the BS, with the Rice factor $K = 2.55 \equiv 4$ dB.

the symbol duration is much smaller than the channel coherence time, $1/f_D$ [23]. Hence, the channel matrix $\boldsymbol{H}(t)$ can be regarded as a random constant matrix $\boldsymbol{H}$ over a long data block. Similar to [11]–[14] and [19], we also assume that $\boldsymbol{H}$ is known to the user, but not at the BS, i.e., there is no transmit beamforming. If the total finite transmitted BS power, $P_{\text{BS, total}}$, is allocated uniformly to all the n_{BS} antennas of the BS array, then the capacity of the MIMO channel in (1), in bits/s/Hz, is given by [1], [2]

$$C = \log_2 \left(\det \left(\mathbf{I}_{n_U} + \frac{P_{\text{BS, total}}}{n_{\text{BS}} P_{\text{noise}}} \boldsymbol{H}\boldsymbol{H}^{\#} \right) \right) \qquad (25)$$

where $\det(\cdot)$ is the determinant. Note that the capacity in (25) is a random variable whose distribution depends on the distribution of the random complex matrix $\boldsymbol{H}\boldsymbol{H}^{\#}$.

For finite values of n_{BS} and n_U and uncorrelated Rayleigh MIMO fading channel (no correlation among the zero-mean complex Gaussian elements of $\boldsymbol{H}$), a simple closed form expression is derived in [1] for $E[C]$. Under the same conditions, plots of the distribution function of C are generated in [2], numerically, via Monte Carlo simulation. Some analytic upper and lower bounds on the MIMO capacity, as well as asymptotic results for large number of antennas are derived in [11], [12], [16], and [19], when the elements of $\boldsymbol{H}$ are correlated. The impact of fading correlation on the MIMO capacity are also studied in [11], [14], and [16]–[19] via Monte Carlo simulations. Some empirical results and measurements are given in [44] and [45].

Here, we consider an example which allows us to study the effect of nonisotropic scattering around the user on the capacity, not addressed in the above references. Suppose the elements of the BS array are far apart from each other and the number of the BS antenna elements is large ($n_{\text{BS}} \to \infty$). Let $\boldsymbol{H} = [\boldsymbol{h}_1 \boldsymbol{h}_2 \ldots \boldsymbol{h}_{n_{\text{BS}}}]$ be the transfer matrix of the Rayleigh channel, where $\boldsymbol{h}_s$ is a $n_U \times 1$ complex zero-mean Gaussian vector, corresponding to the sth BS element, with the common correlation matrix $\Re_U$. Note that the columns of $\boldsymbol{H}$ are independent vectors as the BS antenna elements are far enough from each other.[1] Under these conditions, the sample correlation matrix of set of independent vector observations $\{\boldsymbol{h}_1, \boldsymbol{h}_2, \ldots, \boldsymbol{h}_{n_{\text{BS}}}\}$, i.e., $n_{\text{BS}}^{-1} \boldsymbol{H}\boldsymbol{H}^{\#} = n_{\text{BS}}^{-1} \sum_{s=1}^{n_{\text{BS}}} \boldsymbol{h}_s \boldsymbol{h}_s^{\#}$, converges to $\Re_U$ (see [46, Th. 3.4.4, p. 81]). Therefore, the capacity converges to the nonrandom quantity $\tilde{C}$

$$\tilde{C} = \log_2 \left(\det \left(\boldsymbol{I}_{n_U} + \frac{P_{\text{BS, total}}}{P_{\text{noise}}} \Re_U \right) \right). \qquad (26)$$

For the special case of uncorrelated user's antennas, $\Re_U = I_{n_U}$, (26) reduces to $\tilde{C} = n_U \log_2 (1 + P_{\text{BS, total}}/P_{\text{noise}})$, already given by (6) of [1] and in Appendix C of [47].

Now, we investigate the effect of nonisotropic scattering around the user, parameterized by κ and μ, on the channel capacity in (26), through numerical examples. Suppose both the BS and the user are equipped with linear uniform arrays such that $\delta_{p,p+1} = \delta$ and $d_{l,l+1} = d$, where δ is large, $p = 1, 2, \ldots$, and $l = 1 (n_U = 2)$. Since the total length of the BS array is large, we need the distance D to be very large, to keep the far field assumption meaningful. This makes $\delta\Delta$ very small. Since both arrays are linear, α_{pq} and β_{lm} do not depend on the indices. Assume $\alpha = \beta = 90°$, so the two arrays are parallel. Under these assumptions and for a Rayleigh channel, $K_{1p} = K_{2p} = 0$, $p = 1, 2, \ldots$, the spatial cross-correlation function between the MIMO channel links in (12) simplifies to

$$\rho_{1p,2p}(0) = \frac{I_0\left(\sqrt{\kappa^2 - \frac{4\pi^2 d^2}{\lambda^2} + \frac{j4\pi\kappa \sin(\mu) d}{\lambda}}\right)}{I_0(\kappa)}, \quad p = 1, 2, \ldots \qquad (27)$$

Note that due to the independence of the BS antennas we have $\rho_{1p,2q}(0) = 0$ for $p \neq q$. The temporal version of (27) was first proposed in [8], along with an extensive comparison with

[1]To get an idea on how large the BS elements spacing should be to have the separate BS links uncorrelated, we use (24) which was derived for the MIMO channel example, discussed at the end of the Section IV. Assume that an absolute correlation of 0.15 or less amounts to nearly uncorrelated links. With this in mind and for $K = 0$, $\Delta = 2°$, and $\kappa = 3, 0$ the links $h_{11}(t)$ and $h_{12}(t)$ are almost uncorrelated, provided that $\delta_{12}/\lambda = 15$ and 10, respectively.

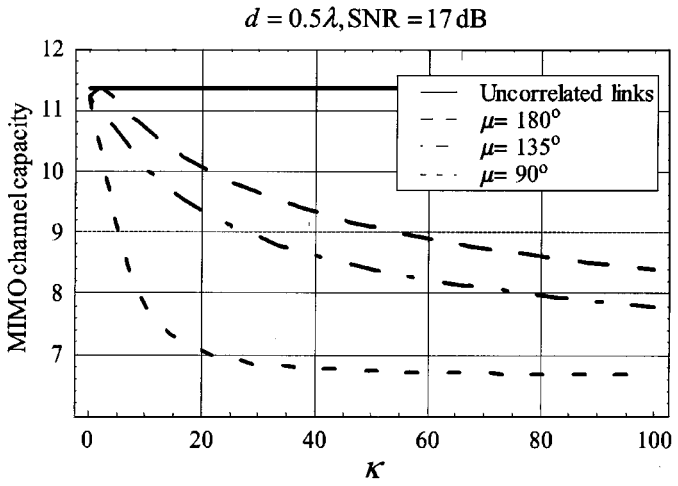

Fig. 7. MIMO channel capacity and nonisotropic scattering around a two element user's array, with an antenna spacing of 0.5λ, different mean directions of signal propagation toward the user (90°, 135°, 180°), 17 dB SNR, and a large linear uniform array at the BS.

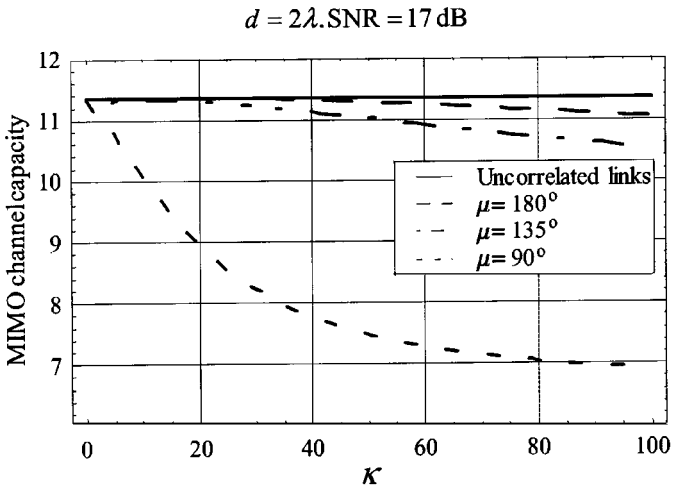

Fig. 8. MIMO channel capacity and nonisotropic scattering around a two element user's array, with an antenna spacing of 2λ, different mean directions of signal propagation toward the user (90°, 135°, 180°), 17 dB SNR, and a large linear uniform array at the BS.

empirical data. In the case of isotropic scattering around the user, $\kappa = 0$, (27) reduces to the Clarke's spatial correlation model $J_0(2\pi d/\lambda)$ [22]. For $P_{\text{BS, total}}/P_{\text{noise}} = 17$ dB, the signal-to-noise ratio, the capacity $\tilde{C}$ in (26) is plotted in Figs. 7 and 8 versus κ, for different mean direction of arrivals μ, and $d = 0.5\lambda$, and $d = 2\lambda$, respectively. The capacity for the case of uncorrelated user's antennas, $2\log_2(1 + P_{\text{BS, total}}/P_{\text{noise}})$, is also plotted in both figures. As is shown in Fig. 7, the capacity decreases as κ increases (smaller angle spread around the user). This decrease is dramatic when the waves impinge the user's array from the inline direction, $\mu = 90°$. As the elements spacing increases from $d = 0.5\lambda$ in Fig. 7 to $d = 2\lambda$ in Fig. 8, the effect of κ on the capacity becomes less pronounced, as the two channel links become less correlated.[2] So, the capacity for the uncorrelated links can be approximately achieved, as is shown in Fig. 8. The inline reception, $\mu = 90°$, still suffers from nonisotropic scattering. This advocates the use of other array configurations such as triangular and hexagonal, which are less sensitive to the mean direction of signal arrival, compared to the linear arrays. Similar results regarding the angle spread and the mean direction of arrival at the BS are observed and discussed in [11].

VI. Conclusion

In this paper, we have proposed a flexible and mathematically tractable space–time cross-correlation function for MIMO frequency nonselective mobile Rice fading channels, where both the BS and the user are equipped with multielement antennas. In our model, the BS receives signal through a narrow angle spread, while the nonuniform distribution for the angle of arrival around the user is modeled by the von Mises distribution, which has previously shown to be successful in describing the measured data. The effect of the Doppler spread for the mobile user is also taken into account. The model also accounts for other parameters of interest such as the distance between the BS and the user, the radius of the ring of local scatterers surrounding the user, and the configuration of the antenna arrays (which might be linear, triangular, etc.). The proposed space–time cross-correlation function is general enough to include well-known special cases for SISO, SIMO, and MISO fading channels, such as Lee's spatio-temporal correlation model and Clarke's classic temporal correlation model. We have used the new model to explore the properties of a widely accepted correlation model for MIMO fading channels. The utility of the new space–time correlation model has also been demonstrated by quantifying the effect of nonisotropic scattering around the user (typical of many outdoor channels) on the capacity of a frequency nonselective time-invariant MIMO Rayleigh fading channel, where the user with linear uniform array receives signals only from a particular direction. Our numerical results show that the capacity decreases as the angle spread seen by the user decreases. Such a loss may be compensated by increasing the distance between the user's array elements, or by employing other array configurations. The impact of the grating lobes on the MIMO capacity, generated by increasing the user's array elements spacing beyond half wavelength, is also discussed. The proposed correlation model provides a useful framework for the analysis and design of multielement antenna systems and space–time modems. For example, the effect of correlated fading on the performance of several space–time coding and detection schemes is investigated in [49] using the new MIMO correlation model, and the contributions of physical channel parameters on the performance are easily quantified.

[2]Of course increasing element spacing beyond half wavelength creates grating lobes in the array directional response [48]. This is not a problem, since diversity, rather than directional discrimination, is the primary mechanism for increasing capacity in the system under consideration [18]. Indeed, the intent is to capture uncorrelated copies of the signal from all irections of the rich scattering environment.

Acknowledgment

A. Abdi expresses his gratitude to Dr. D. S. Shiu at Qualcomm, Dr. D. Chizhik at Lucent Technologies, Prof. I. E. Telatar

at Ecole Polytechnique Federale de Lausanne, and Prof. J. C. Kieffer at the University of Minnesota, for useful discussions regarding the channel capacity.

REFERENCES

[1] I. E. Telatar, "Capacity of multi-antenna Gaussian channels," *European Trans. Telecommun. Related Technol.*, vol. 10, pp. 585–595, 1999.

[2] G. J. Foschini and M. J. Gans, "On limits of wireless communications in a fading environment when using multiple antennas," *Wireless Pers. Commun.*, vol. 6, pp. 311–335, 1998.

[3] V. Tarokh, N. Seshadri, and A. R. Calderbank, "Space-time codes for high data rate wireless communication: Performance criterion and code construction," *IEEE Trans. Inform. Theory*, vol. 44, pp. 744–765, 1998.

[4] J. Fuhl, J. P. Rossi, and E. Bonek, "High-resolution 3-D direction-of-arrival determination for urban mobile radio," *IEEE Trans. Antennas Propagat.*, vol. 45, pp. 672–682, 1997.

[5] P. C. Fannin and A. Molina, "Analysis of mobile radio channel sounding measurements in inner city Dublin at 1.808 GHz," *Proc. Inst. Elect. Eng Commun.*, vol. 143, pp. 311–316, 1996.

[6] A. Abdi and M. Kaveh, "A versatile spatio-temporal correlation function for mobile fading channels with nonisotropic scattering," in *Proc. IEEE Workshop Statistical Signal Array Processing*, Pocono Manor, PA, 2000, pp. 58–62.

[7] ——, "Parametric modeling and estimation of the spatial characteristics of a source with local scattering," presented at the IEEE Int. Conf. Acoustics, Speech, and Signal Processing, Orlando, FL, 2002.

[8] A. Abdi, J. A. Barger, and M. Kaveh, "A parametric model for the distribution of the angle of arrival and the associated correlation function and power spectrum at the mobile station," *IEEE Trans. Veh. Technol.*, to be published.

[9] T. A. Chen, M. P. Fitz, W. Y. Kuo, M. D. Zoltowski, and J. H. Grimm, "A space-time model for frequency nonselective Rayleigh fading channels with applications to space-time modems," *IEEE J. Select. Areas Commun.*, vol. 18, pp. 1175–1190, 2000.

[10] A. F. Naguib, V. Tarokh, N. Seshadri, and A. R. Calderbank, "A space-time coding modem for high-data-rate wireless communications," *IEEE J. Select. Areas Commun.*, vol. 16, pp. 1459–1478, 1998.

[11] D. S. Shiu, G. J. Foschini, M. J. Gans, and J. M. Kahn, "Fading correlation and its effect on the capacity of multielement antenna systems," *IEEE Trans. Commun.*, vol. 48, pp. 502–513, 2000.

[12] A. M. Sengupta and P. P. Mitra, "Capacity of Multivariate Channels With Multiplicative Noise: I. Random Matrix Techniques and Large-N Expansions for Full Transfer Matrices," Bell Labs., 2000.

[13] A. L. Moustakas, H. U. Baranger, L. Balents, A. M. Sengupta, and S. H. Simon, "Communication through a diffusive medium: Coherence and capacity," *Science*, vol. 287, pp. 287–290, 2000.

[14] D. Chizhik, F. R. Farrokhi, J. Ling, and A. Lozano, "Effect of antenna separation on the capacity of BLAST in correlated channels," *IEEE Commun. Lett.*, vol. 4, pp. 337–339, 2000.

[15] D. Chizhik, G. J. Foschini, and R. A. Valenzuela, "Capacities of multi-element transmit and receive antennas: Correlations and keyholes," *Electron. Lett.*, vol. 36, pp. 1099–1100, 2000.

[16] A. Gorokhov, "Transmit diversity versus SDMA: Analytic and numerical comparisons," in *Proc. IEEE Int. Conf. Communications*, New Orleans, LA, 2000, pp. 1020–1024.

[17] K. I. Pedersen, J. B. Andersen, J. P. Kermoal, and P. Mogensen, "A stochastic multiple-input–multiple-output radio channel model for evaluation of space-time coding algorithms," in *Proc. IEEE Vehic. Technol. Conf.*, Boston, MA, 2000, pp. 893–897.

[18] P. F. Driessen and G. J. Foschini, "On the capacity formula for multiple input–multiple output wireless channels: A geometric interpretation," *IEEE Trans. Commun.*, vol. 47, pp. 173–176, 1999.

[19] C. N. Chuah, J. M. Kahn, and D. Tse, "Capacity of multi-antenna array systems in indoor wireless environment," in *Proc. IEEE Global Telecommunications Conf.*, Sydney, Australia, 1998, pp. 1894–1899.

[20] J. Salz and J. H. Winters, "Effect of fading correlation on adaptive arrays in digital mobile radio," *IEEE Trans. Veh. Technol.*, vol. 43, pp. 1049–1057, 1994.

[21] B. H. Fleury, "First- and second-order characterization of direction dispersion and space selectivity in the radio channel," *IEEE Trans. Inform. Theory*, vol. 46, pp. 2027–2044, 2000.

[22] W. C. Jakes Jr, "Multipath interference," in *Microwave Mobile Communications*, W. C. Jakes Jr., Ed. New York: Wiley, 1974, pp. 11–78.

[23] G. L. Stuber, *Principles of Mobile Communication*. Boston, MA: Kluwer, 1996.

[24] W. C. Y. Lee, "Effects on correlation between two mobile radio base-station antennas," *IEEE Trans. Commun.*, vol. 21, pp. 1214–1224, 1973.

[25] S. Roy and D. D. Falconer, "Modeling the narrowband base station correlated diversity channel," in *Proc. IEEE Commun. Theory Mini-Conf.*, Vancouver, BC, Canada, 1999, pp. 89–95.

[26] S. P. Stapleton, X. Carbo, and T. McKeen, "Tracking and diversity for a mobile communications base station array antenna," in *Proc. IEEE Vehic. Technol. Conf.*, Atlanta, GA, 1996, pp. 1695–1699.

[27] K. I. Pedersen, P. E. Mogensen, and B. H. Fleury, "A stochastic model of the temporal and azimuthal dispersion seen at the base station in outdoor propagation environments," *IEEE Trans. Vehic. Technol.*, vol. 49, pp. 437–447, 2000.

[28] U. Martin, "Spatio-temporal radio channel characteristics in urban macrocells," *IEE Proc. Radar, Sonar, Navig.*, vol. 145, pp. 42–49, 1998.

[29] P. Pajusco, "Experimental characterization of D.O.A at the base station in rural and urban area," in *Proc. IEEE Veh. Technol. Conf.*, Ottawa, ON, Canada, 1998, pp. 993–997.

[30] T. S. Chu and L. J. Greenstein, "A semi-empirical representation of antenna diversity gain at cellular and PCS base stations," *IEEE Trans. Commun.*, vol. 45, pp. 644–646, 1997.

[31] F. Adachi, M. T. Feeney, A. G. Williamson, and J. D. Parsons, "Cross-correlation between the envelopes of 900 MHz signals received at a mobile radio base station site," *IEE Proc. F, Commun., Radar, Signal Processing*, vol. 133, pp. 506–512, 1986.

[32] C. Tepedelenlioglu, A. Abdi, G. Giannakis, and M. Kaveh, "Estimation of Doppler spread and signal strength in mobile communications with applications to handoff and adaptive transmission," *Wireless Commun. Mob. Comput.*, vol. 1, pp. 221–242, 2001.

[33] Y. C. Ko, A. Abdi, M. S. Alouini, and M. Kaveh, "Average outage duration of diversity systems over generalized fading channels," in *Proc. IEEE Wireless Commun. Networking Conf.*, Chicago, IL, 2000, pp. 216–221.

[34] I. S. Gradshteyn and I. M. Ryzhik, *Table of Integrals, Series, and Products*, 5th ed, A. Jeffrey, Ed. San Diego, CA: Academic, 1994.

[35] M. Stege, J. Jelitto, M. Bronzel, and G. Fettweis, "A multiple input–multiple output channel model for simulation of TX- and RX-diversity wireless systems," in *Proc. IEEE Vehic. Technol. Conf.*, Boston, MA, 2000, pp. 833–839.

[36] W. C. Y. Lee, "Level crossing rates of an equal-gain predetection diversity combiner," *IEEE Trans. Commun. Technol.*, vol. 18, pp. 417–426, 1970.

[37] T. Fulghum and K. Molnar, "The Jakes fading model incorporating angular spread for a disk of scatterers," in *Proc. IEEE Vehic. Technol. Conf.*, Ottawa, ON, Canada, 1998, pp. 489–493.

[38] H. Masui, M. Ishii, K. Sakawa, H. Shimizu, T. Kobayashi, and M. Akaike, "Microwave spatio-temporal channel characteristics measured at base station in an urban environment," in *Proc. IEEE Vehic. Technol. Conf.*, Boston, MA, 2000, pp. 829–832.

[39] J. Fuhl, A. F. Molisch, and E. Bonek, "Unified channel model for mobile radio systems with smart antennas," *IEE Proc. Radar, Sonar, Navig.*, vol. 145, pp. 32–41, 1998.

[40] R. Janaswamy, *Radiowave Propagation and Smart Antennas for Wireless Communications*. Boston, MA: Kluwer, 2001.

[41] L. Schumacher, K. I. Pedersen, J. P. Kermoal, and P. Mogensen, "A link-level MIMO radio channel simulator for evaluation of combined transmit/receive diversity concepts within the METRA project," in *Proc. IST Mobile Commun. Summit*, Galway, Ireland, 2000, pp. 515–520.

[42] A. K. Gupta and T. Varga, *Elliptically Contoured Models in Statistics*. Dordrecht, The Netherlands: Kluwer, 1993.

[43] H. H. Andersen, M. Hojbjerre, D. Sorensen, and P. S. Eriksen, "Linear and graphical models for the multivariate complex normal distribution," in *Lecture Notes in Statistics*. New York: Springer, 1995, vol. 101.

[44] C. C. Martin, J. H. Winters, and N. R. Sollenberger, "Multiple-input multiple-output (MIMO) radio channel measurements," in *Proc. IEEE Vehicular Technolology Conf.*, Boston, MA, 2000, pp. 774–779.

[45] J. P. Kermoal, P. E. Mogensen, S. H. Jensen, J. B. Andersen, F. Frederiksen, T. B. Sorensen, and K. I. Pedersen, "Experimental investigation of multipath richness for multi-element transmit and receive antenna arrays," in *Proc. IEEE Vehiccular Technology Conf.*, Tokyo, Japan, 2000, pp. 2004–2008.

[46] T. W. Anderson, *An Introduction to Multivariate Statistical Analysis*, 2nd ed. New York: Wiley, 1984.

[47] T. L. Marzetta and B. M. Hochwald, "Capacity of a mobile multiple-antenna communication link in Rayleigh flat fading," *IEEE Trans. Inform. Theory*, vol. 45, pp. 139–157, 1999.

[48] D. H. Johnson and D. E. Dudgeon, *Array Signal Processing: Concepts and Techniques*. Englewood Cliffs, NJ: Prentice-Hall, 1993.

[49] M. O. Damen, A. Abdi, and M. Kaveh, "On the effect of correlated fading on several space-time coding and detection schemes," in *Proc. IEEE Vehicular Technology Conf.*, Atlantic City, NJ, 2001, pp. 13–16.

Ali Abdi (S'98–M'01) received the Ph.D. degree in electrical engineering from the University of Minnesota, Minneapolis, MN, in 2001.

He joined the Department of Electrical and Computer Engineering of New Jersey Institute of Technology (NJIT), Newark, NJ, in the Fall of 2001, as an Assistant Professor. His previous research interests have included stochastic processes, wireless communications, pattern recognition, neural networks, and time series analysis. His current work is mainly focused on different aspects of wireless communications, with special emphasis on channel modeling and estimation, multiantenna systems, and system performance evaluation.

Mostafa Kaveh (S'73–M'75–SM'83–F'88) received the B.S. and Ph.D. degrees from Purdue University, Lafayette, IN, in 1969 and 1974, respectively, and the M.S. degree from the University of California at Berkeley, in 1970.

He has been at the University of Minnesota, since 1975, where he is a Professor and, since 1990, the Head of the Department of Electrical and Computer Engineering. He was a Design Engineer at Scala Radio Corp., San Leadndro, CA, 1970, and has consulted for industry, including the MIT Lincoln Laboratory, 3M, and Honeywell.

Dr. Kaveh has been professionally active in the Signal Processing Society of the Institute for Electrical and Electronic Engineers (IEEE), which he has served as the Vice President for Publications, a member of the Board of Governors, and the General Chair of ICASSP93. He was the recipient (with A. Barabell) of a 1986 ASSP Senior (best paper) Award, the 1988 ASSP Meritorious Service Award, an IEEE Third Millennium Medal in 2000, and the 2000 Society Award from the IEEE Signal Processing Society.